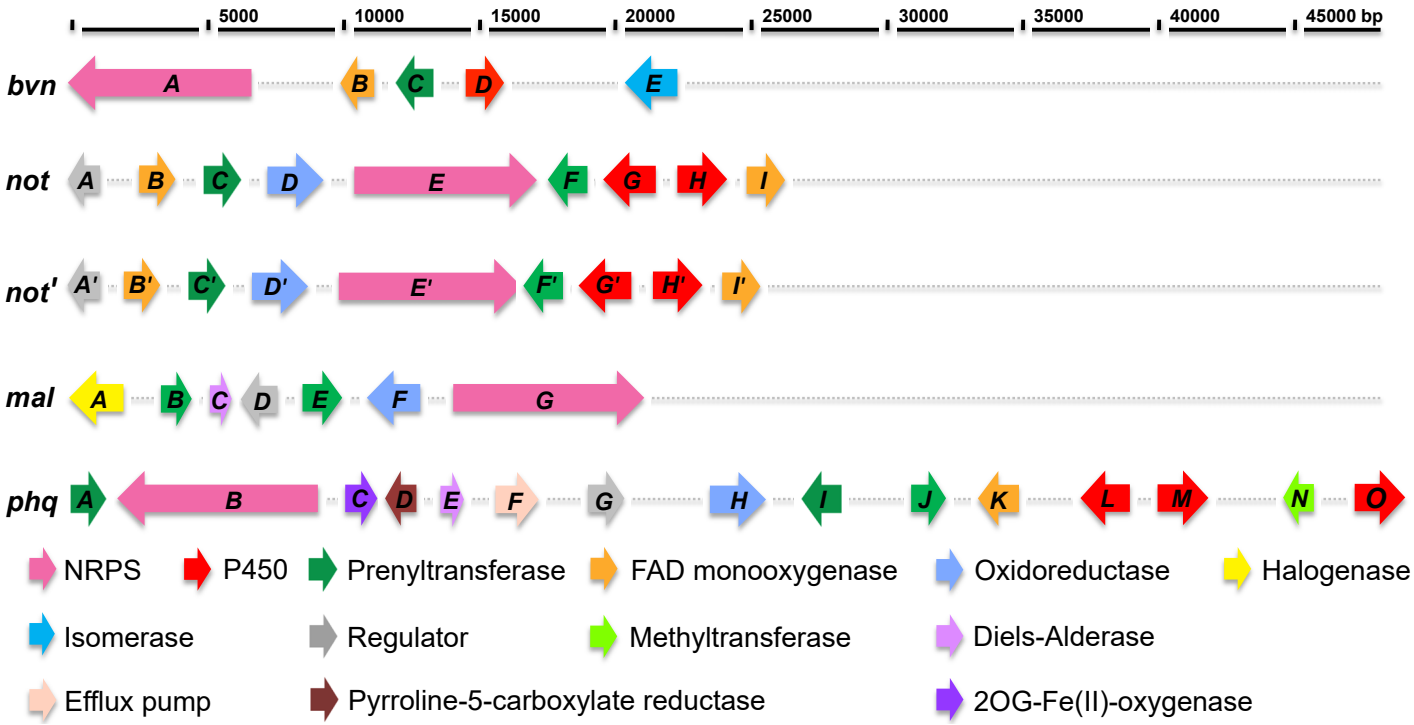

Figure S1. Comparative biosynthetic gene clusters for bicyclo[2.2.2]diazaoctane fungal indole alkaloids, including brevianamide (*bvn*), notoamide (*not/not'*), malbrancheamide (*mal*), and paraherquamide (*phq*).

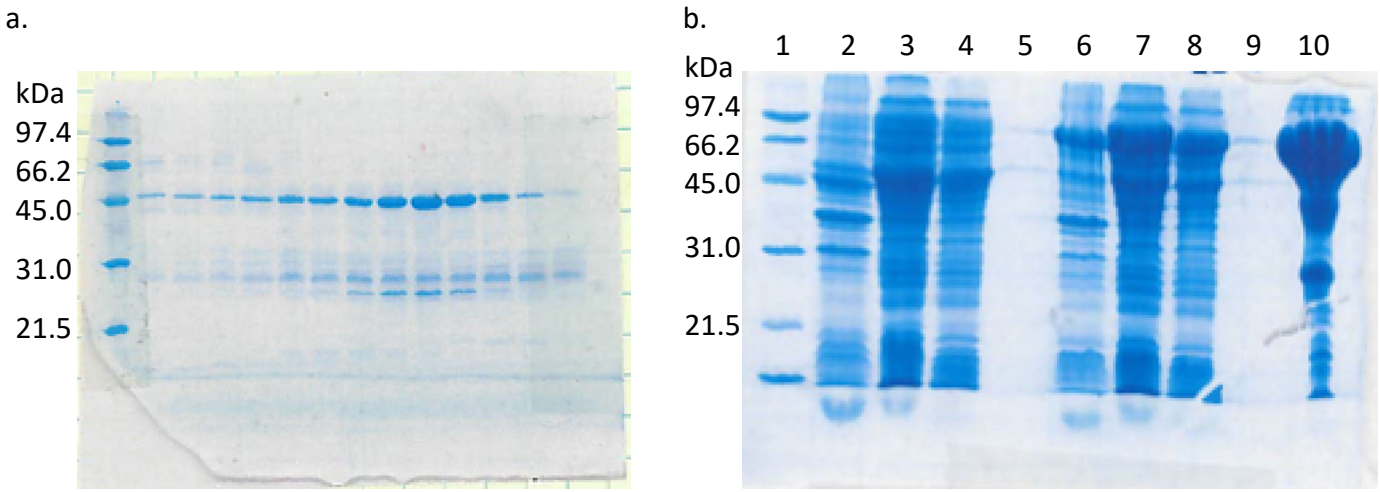

Figure S2. SDS-PAGE gels from purification of a.) NotI (47,044 Da) and b.) MBP-NotI′ (89,544 Da). NotI was purified via a gradient elution with increasing concentrations of imidazole to yield ~ 42 mg of protein per liter of expression culture. NotI′ was fused to an N-terminal MBP tag and batch purified resulting in 15 mg of protein per liter of expression culture. Columns 2-5 represent an attempt to express NotI′ in the pTrc vector, while the MBP-fusion resulted in majority soluble protein (columns 7 supernatent and 10 elution with 250 mM imidazole) and some insoluble protein (column 6 cell debri pellet and 8 flowthrough from the Ni column).

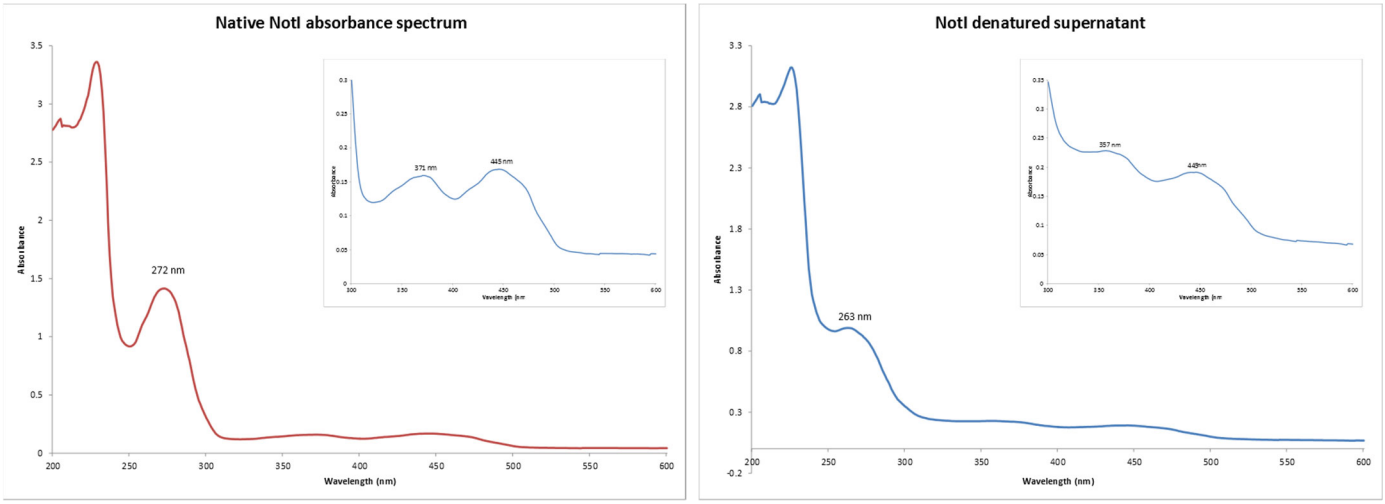

Figure S3. UV-Vis spectra of purified NotI protein solution (left) and the supernatant of denatured NotI protein solution (right). Denatured protein was generated by boiling for 15 minutes. The flavin cofactor peaks at 360 and 450 nm are present in both the native protein solution and the denatured supernatant.

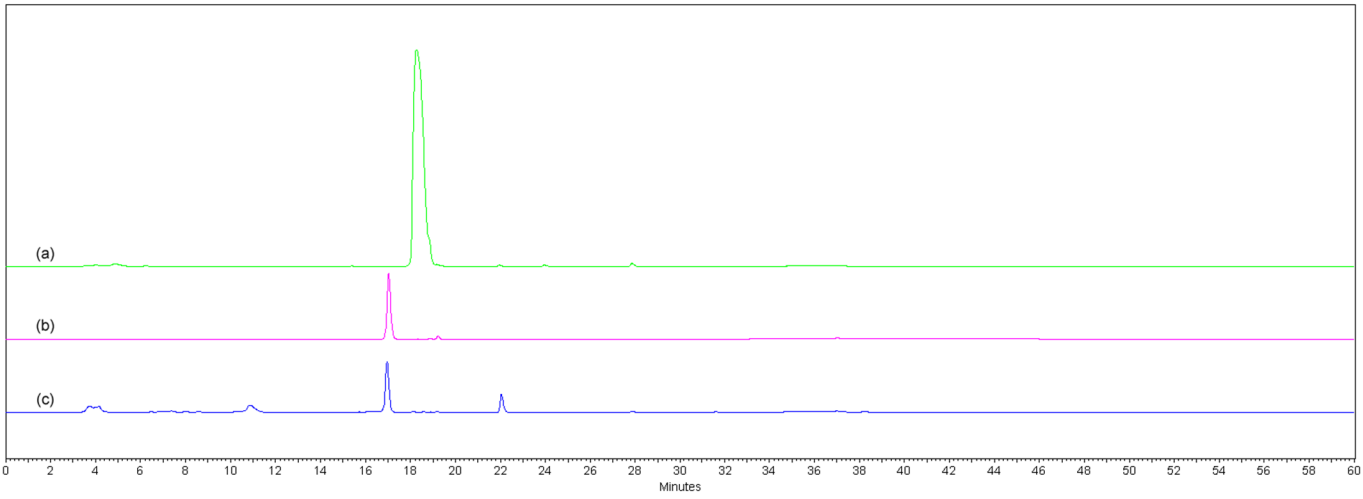

Figure S4. Identification of FAD as the non-covalently bound NotI flavin cofactor. (a) FMN standard; (b) FAD standard; (c) NotI supernatant after denaturation of protein by boiling and centrifugation.

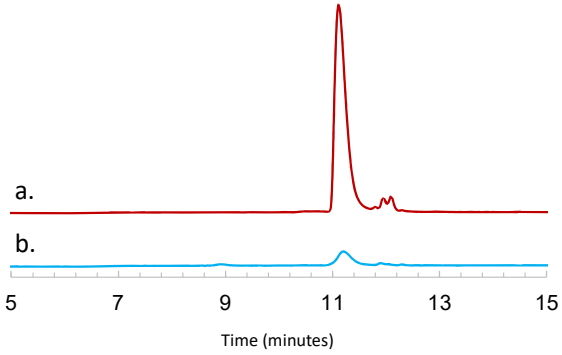

Figure S5. Identification of FAD as the non-covalently bound NotI′ flavin cofactor by HPLC monitored at 448nm. (a) FAD standard; (b) NotI′ supernatant after denaturation of protein by boiling and centrifugation.

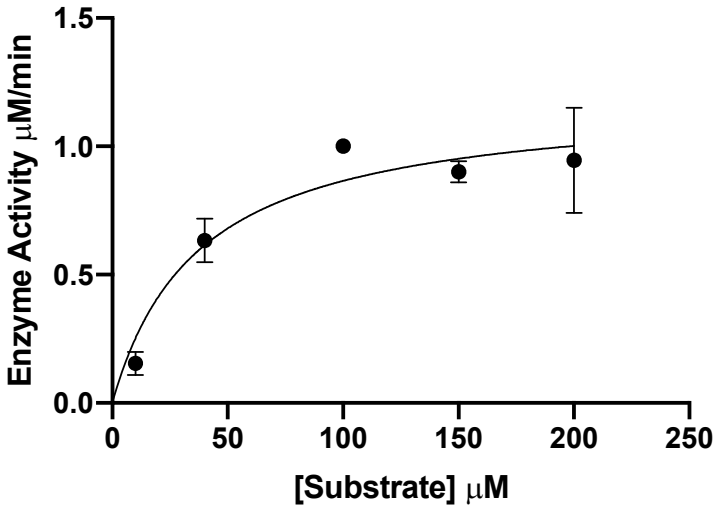

Figure S6. Kinetic curve of NotI against (-)-stephacidin A (**4**).

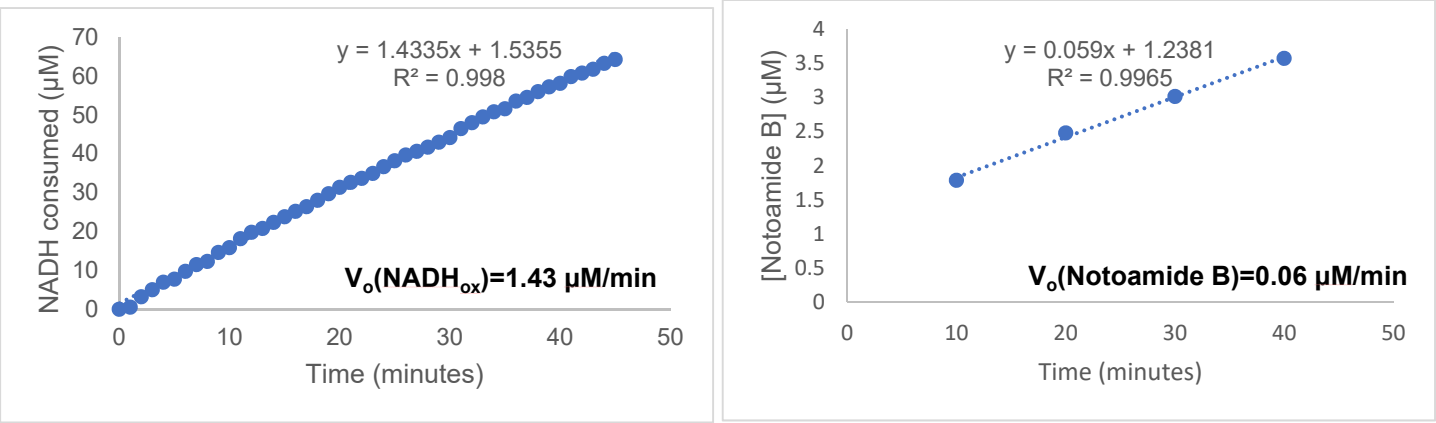

Figure S7. Comparison of the rate of NADH oxidation and the average rate of product formation in a reaction with NotI and (-)-stephacidin A (**4**). The higher rate of NADH oxidation indicates decoupling of these two catalytic factors, and the epoxidation efficiency is 4.1%.

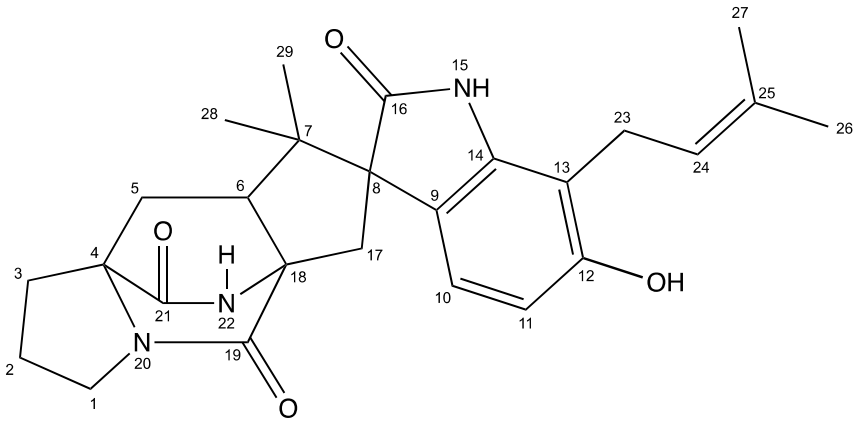

Figure S8. Numbering scheme for notoamide TI (**18**).

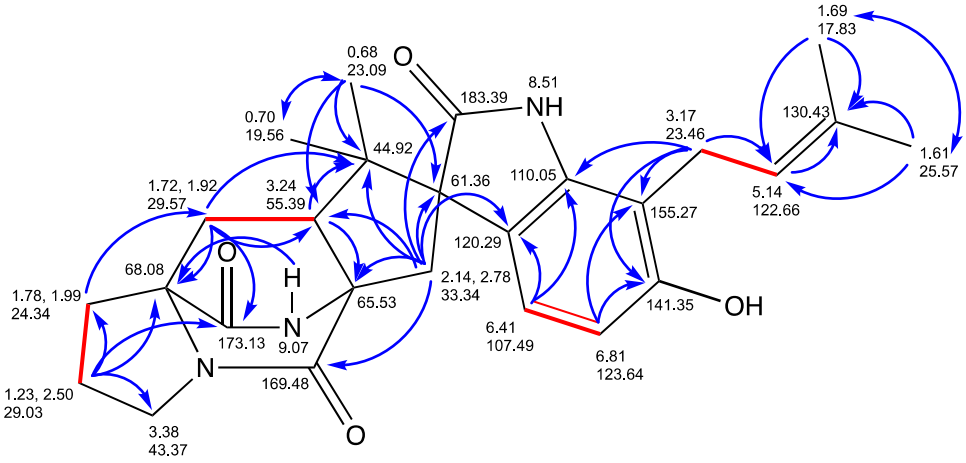

Figure S9. Planar structure of Notoamide TI (**18**) showing gCOSY correlations with bold red bonds and gHMBCAD correlations with blue arrows recorded at 700 MHz in $(CD_3)_2SO$-d_6.

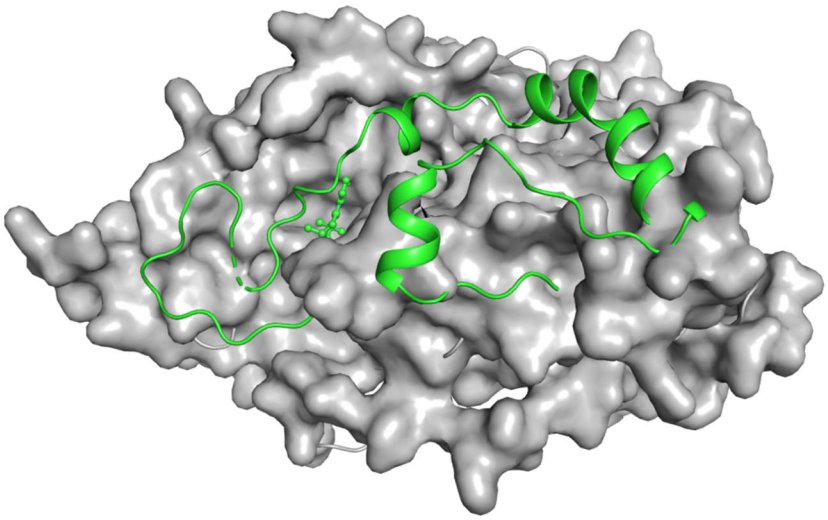

Figure S10. C-terminus and substrate paraherquamide L from PhqK crystal structure (green, PDB ID: 6pvi) aligned with the surface representation of the NotI homology model.

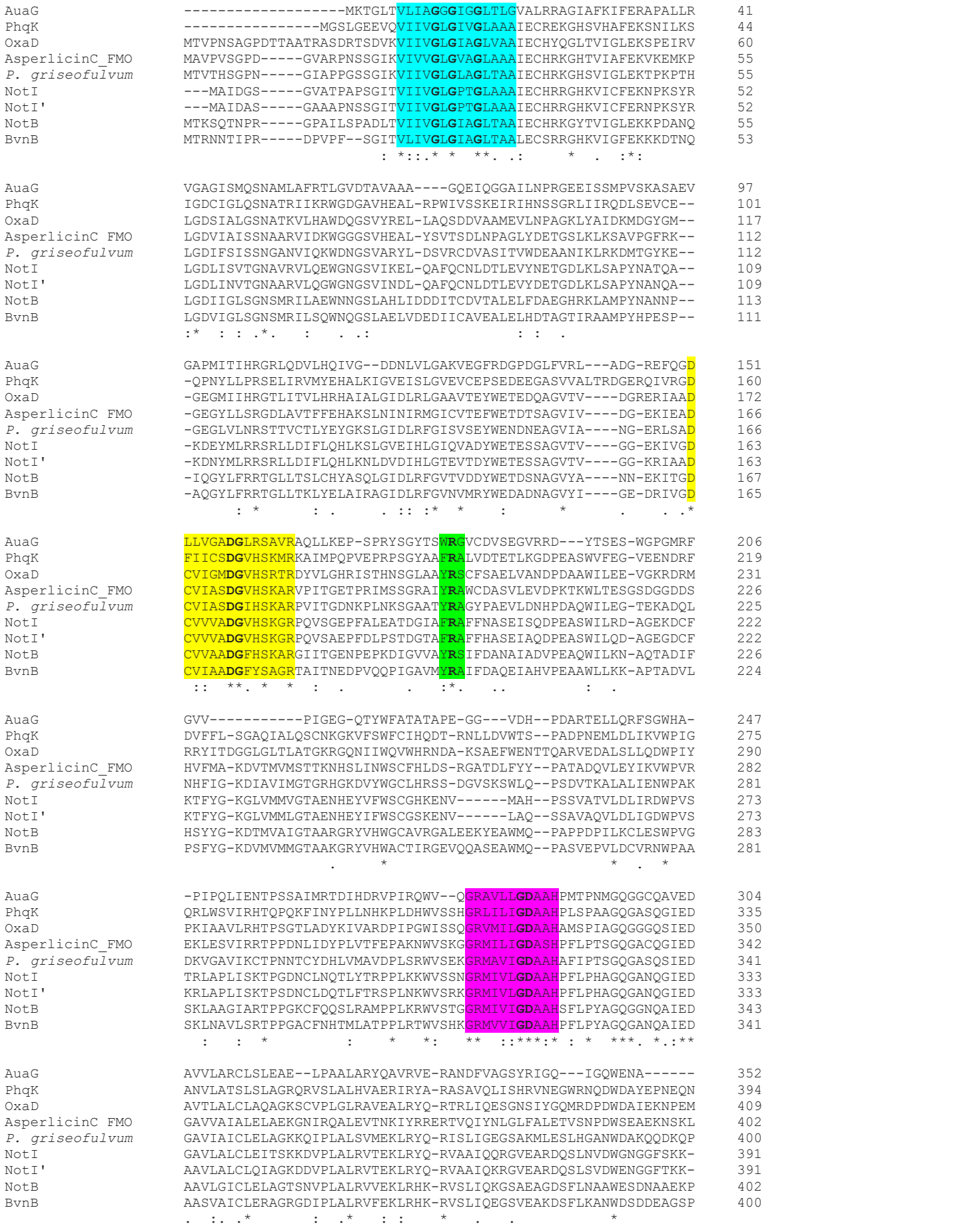
AuaG
PhqK
OxaD
AsperlicinC_FMO
P. griseofulvum
NotI
NotI'
NotB
BvnB

```
AuaG                -----FACWVREKLMRMMSSDRVD---ARTRRNLQFTPL----------------------     383
PhqK                IASLPLETWIYGHDSQAYTEQEFEMVVRAVQEGEEYHATNLPDKLRVQLG--IRNVDVKE     452
OxaD                I-KFPRPQWIFGYDARRDVSEEFPTVKKAIEEGSEYRPRNIPEDCQYQIVHDYKKTVST-     467
AsperlicinC FMO     F-AIPNPEWVLNHNCQKSAYDEYHKIAESIANGTEYTPQNIPSSAVRS------------     449
P. griseofulvum     T-LIARAMWIFDHDCQKSTYEEFEKAAEAVVSGSTYVPANIPNDGRHGIVEEEGKSTVKV     459
NotI                --LTLHPAWLHDHDCIKQVYEEFDKAADAVTKGHEHTFGGIPVG----------------     433
NotI'               --LTLYPAWLHDQDCIKQVYEEFDKAVAAVTKGHECTFGGIPVD----------------     433
NotB                T-AFTHQAWVYAHNCVDHAYEQFNAAAEAVMNGWEYTPTNIPANGKFRQEEG--NI----     455
BvnB                S-AYLHQSWVYNHDCVQHVVEEFQTAADAIRHGRKYIPTNVPVDGKYRQE----------     449
                           *:          :.          .

AuaG                -----------      383
PhqK                PLQNKSP----      459
OxaD                -----------      467
AsperlicinC FMO     -----------      449
P. griseofulvum     PSAHSAPISAE      470
NotI                -----------      433
NotI'               -----------      433
NotB                -----------      455
BvnB                -----------      449
```

Figure S11. Sequence alignment of flavin-dependent monooxygenases (FMOs) including AuaG,[1] PhqK,[2] OxaD,[3] asperlicin C monooxygenase (GenBank: GBF62818.1), FMO from *Penicillium griseofulvum* (GenBank: KXG49074.1), NotI, NotI′, NotB,[4], and BvnB[5] performed using Clustal2.1.[6] The proposed catalytic arginine is highlighted in bold in the green section. The first FAD-binding motif or the Rossmann fold (*βαβ*-fold, containing GxGxxG) is shown highlighted in cyan, the second FAD-binding motif (GD sequence) is shown highlighted in magenta, and the DG motif is highlighted in yellow.[7]

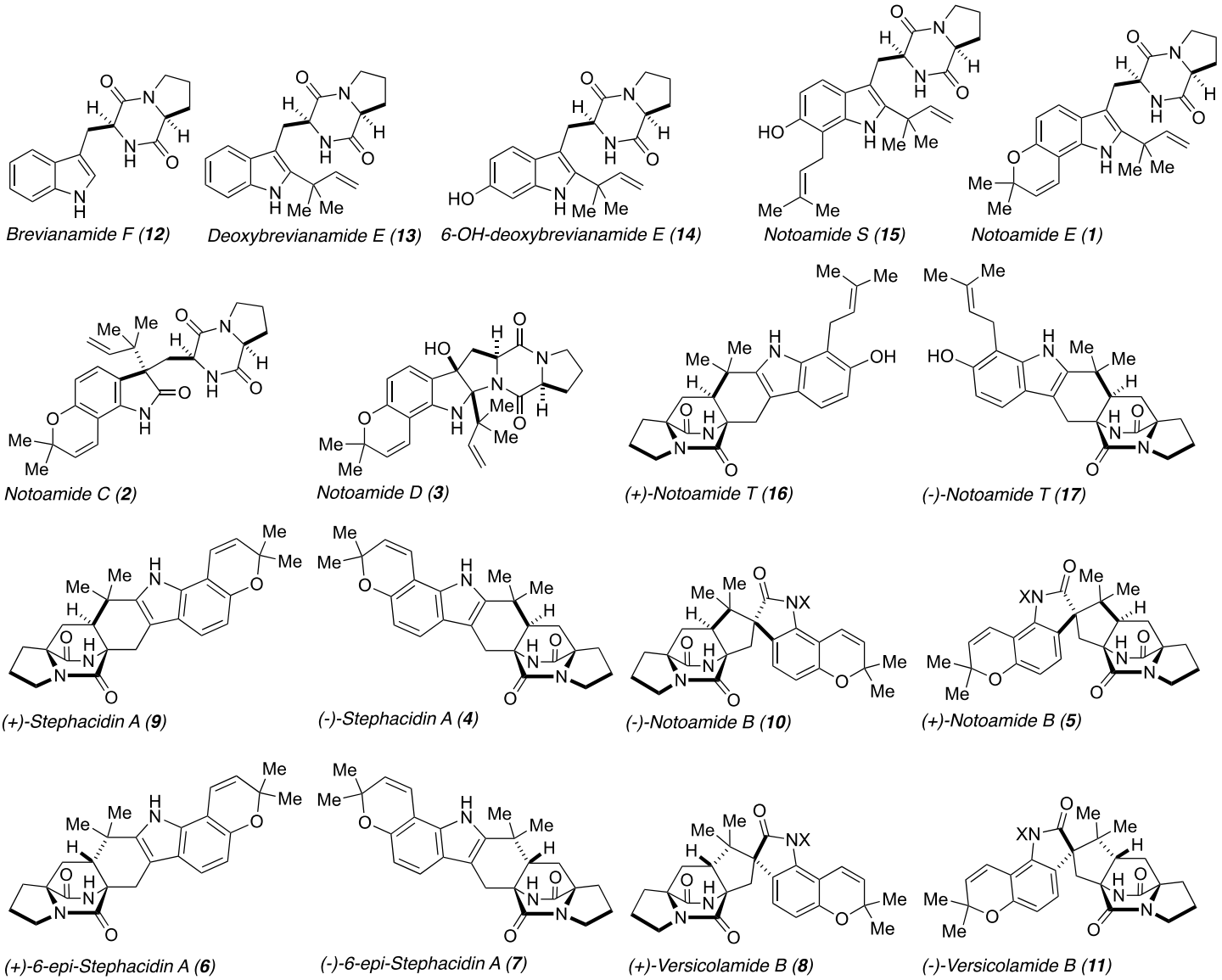

Figure S12. Substrates and products from reactions with NotI and NotI′. (-)-versicolamide B (**11**) has not been isolated from *Aspergillus amoenus* or *Aspergillus protuberus*.

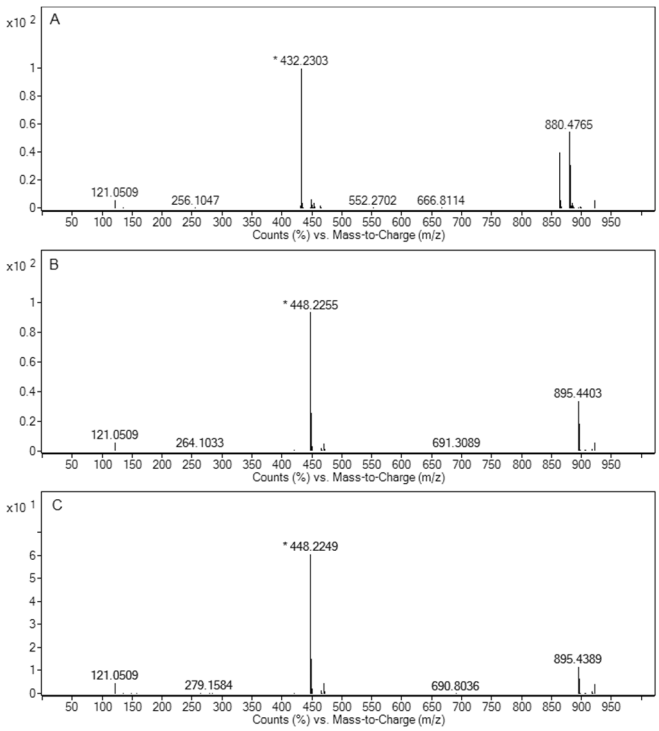

Figure S13. Mass spectra (MS) of (A) (-)-stephacidin A (**4**), expected $[M+H]^+$ = 432.2287; (B) (+)-notoamide B (**5**) formed from reaction with NotI, expected $[M+H]^+$ = 448.2236; (C) (+)-notoamide B (**5**) formed from reaction with NotI′), expected $[M+H]^+$ = 448.2236. Data were measured on an Agilent Q-TOF LC-MS.

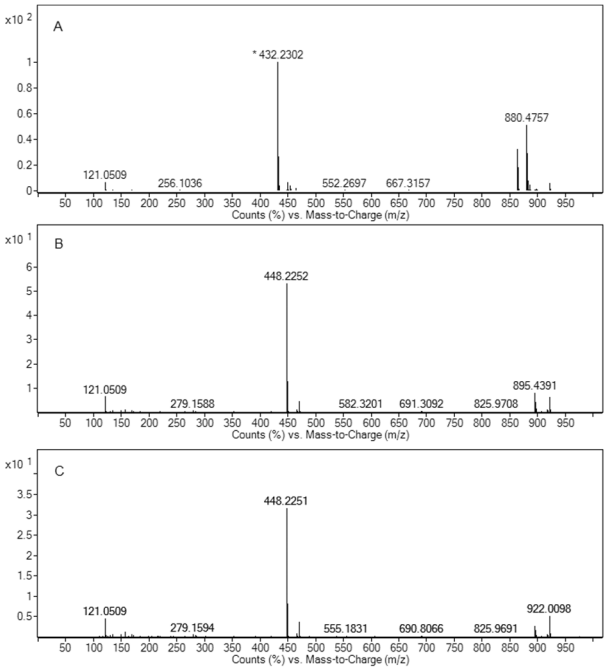

Figure S14. Mass spectra of (A) (+)-stephacidin A (**9**) standard expected $[M+H]^+$ = 432.2287; (B) (-)-notoamide B (**10**) produced by NotI, expected $[M+H]^+$ = 448.2236; (C) (-)-notoamide B (**10**) produced by NotI′ expected $[M+H]^+$ = 448.2236. Data were measured on an Agilent Q-TOF LC-MS.

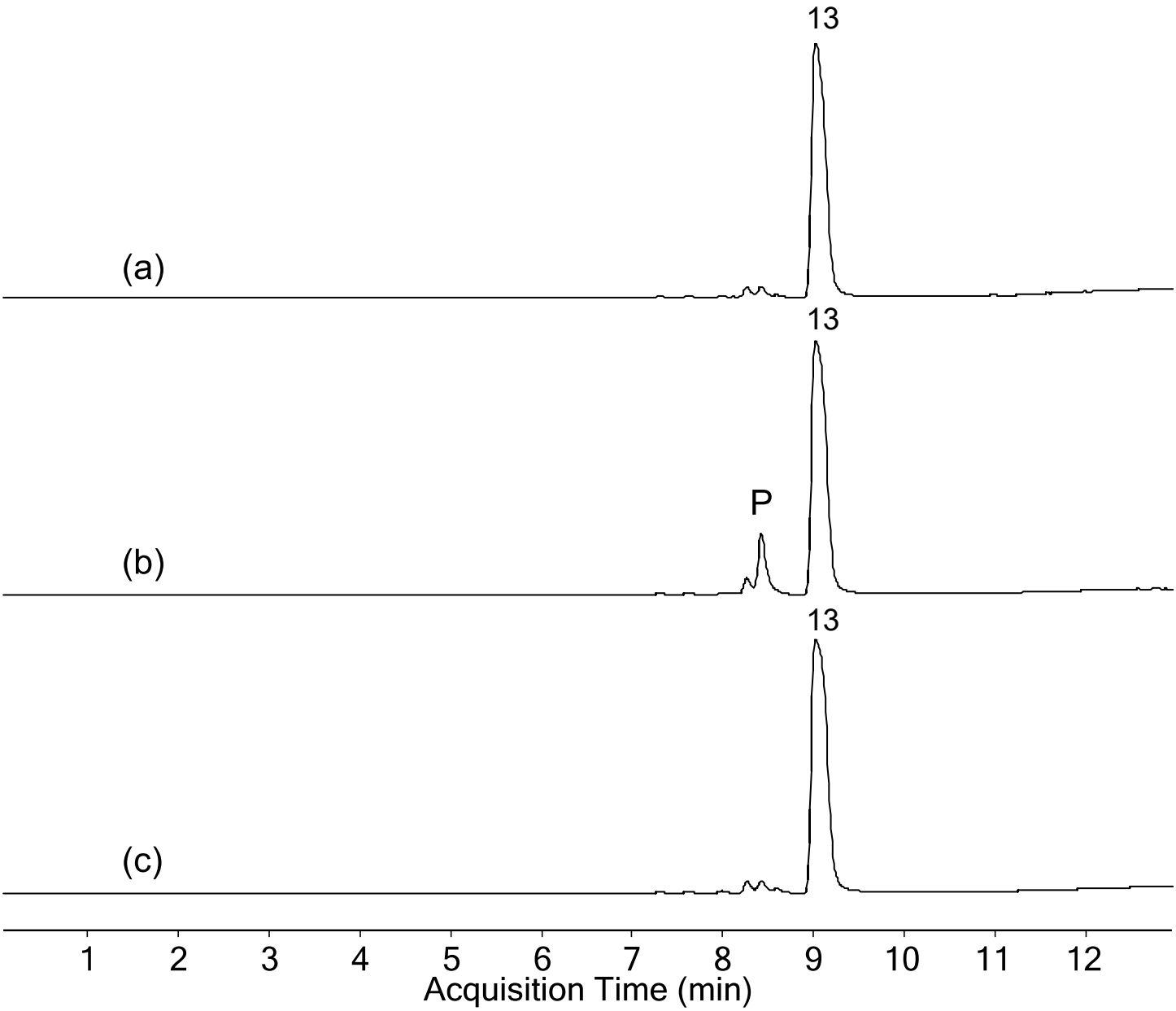

Figure S15. Q-TOF LC-MS analysis depicting EICs of (a) NotI′ reaction with deoxybrevianamide E (**13**); (b) NotI reaction with **13**; (c) no enzyme control with **13**. Product formed is denoted with **P**. Data were measured on an Agilent Q-TOF LC-MS.

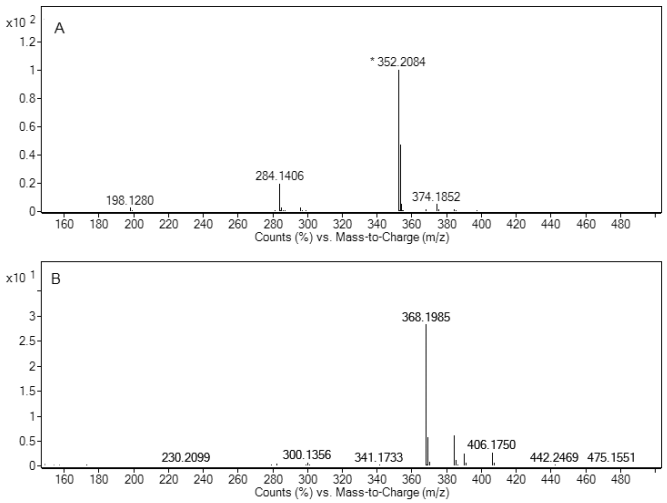

Figure S16. Mass spectra of (A) deoxybrevianamide E (**13**) standard, expected $[M+H]^+$ = 352.2025; (B) Product formed from NotI reaction with **13**, expected $[M+H]^+$ = 368.1974. Data were measured on an Agilent Q-TOF LC-MS.

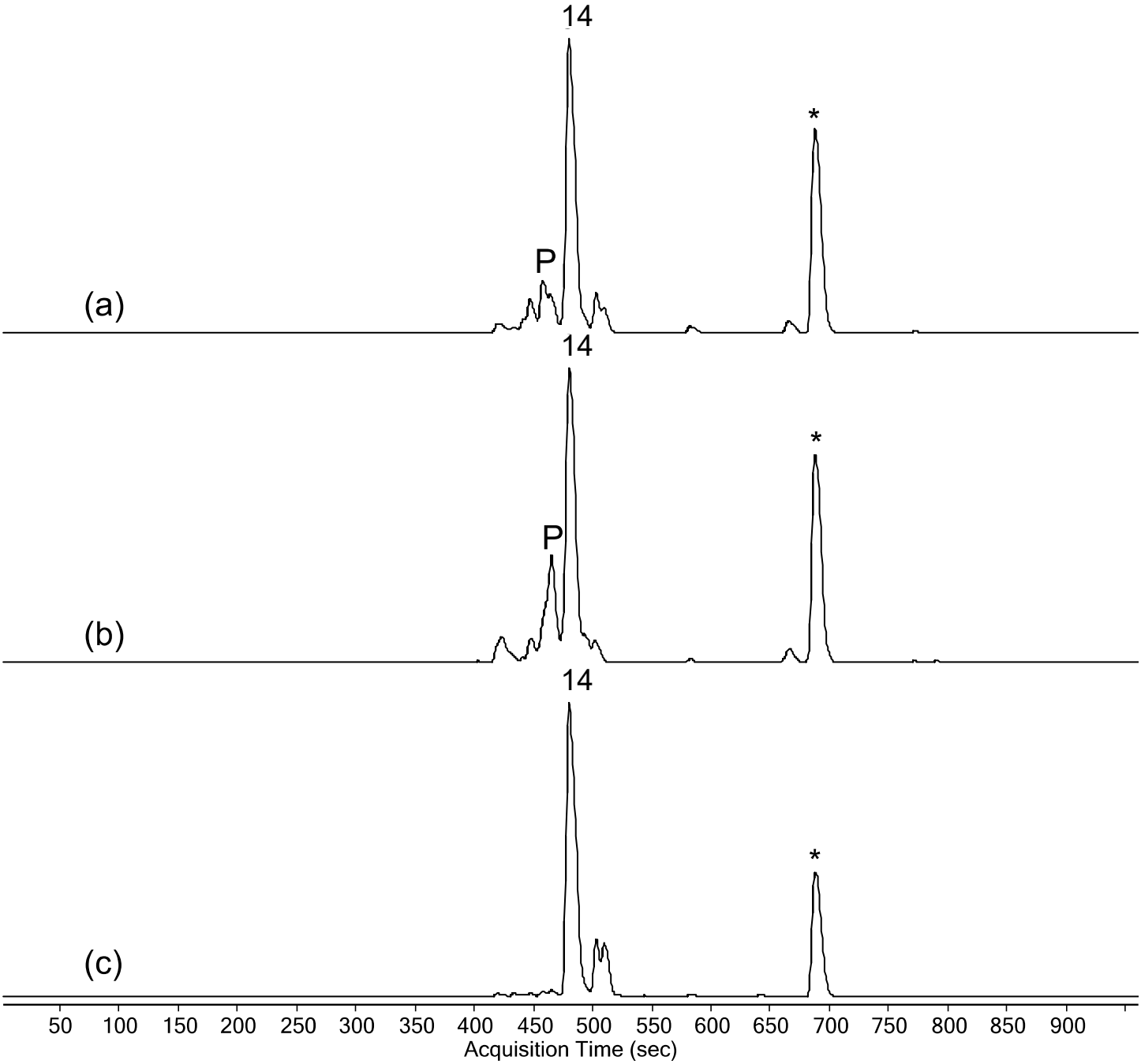

Figure S17. Q-TOF LC-MS analysis depicting EICs of (a) NotI′ reaction with 6-OH-deoxybrevianamide E (**14**); (b) NotI reaction with **14**; (c) no enzyme control with **14**. Products formed are denoted with **P**. Asterisk denotes a possible diastereomer of **14**. Data were measured on an Agilent Q-TOF LC-MS.

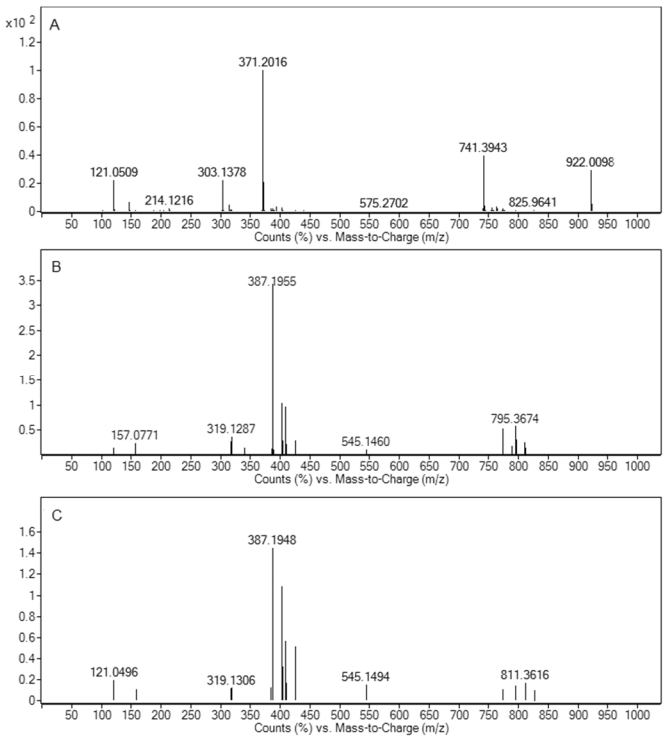

Figure S18. Mass spectra of (A) 6-OH-deoxybrevianamide E (**14**) standard labelled with three ^{13}C atoms, expected $[M+H]^+$ = 371.1974; (B) Product formed from NotI reaction with **14**, expected $[M+H]^+$ = 387.1923; (C) Product formed from NotI′ reaction with **14**, expected $[M+H]^+$ = 387.1923. Data were measured on an Agilent Q-TOF LC-MS.

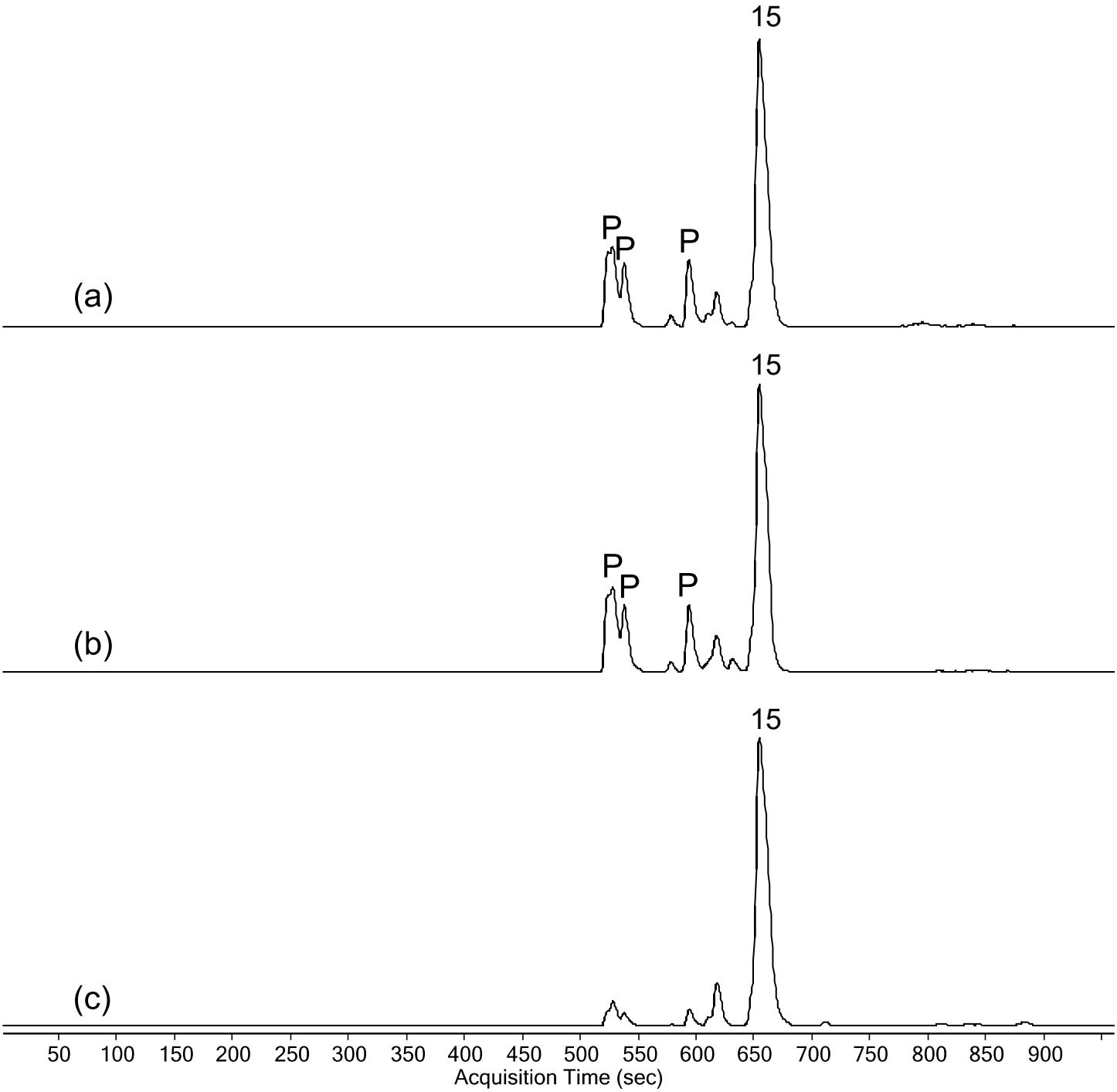

Figure S19. Q-TOF LC-MS analysis depicting EICs of (a) NotI′ reaction with notoamide S (**15**); (b) NotI reaction with **15**; (c) no enzyme control with **15**. Product(s) formed are denoted with **P**. Data were measured on an Agilent Q-TOF LC-MS.

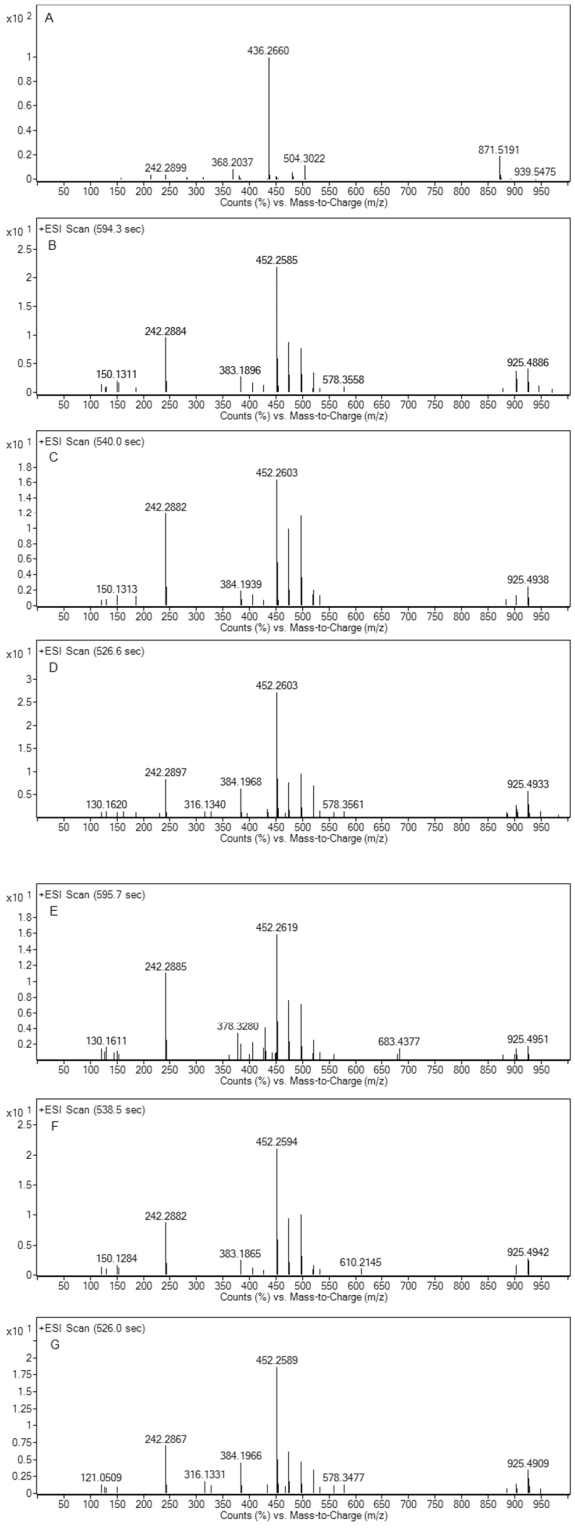

Figure S20. Mass spectra of (A) notoamide S (**15**) standard, expected $[M+H]^+$ = 436.2600; (B) Product formed from reaction of NotI with **15** observed at 594.3 seconds; (C) Product formed from reaction of NotI with **15** observed at 540.0 seconds; (D) Product formed from reaction of NotI with **15** observed at 526.6 seconds; (E) Product formed from reaction of NotI′ with **15** observed at 595.7 seconds; (F) Product formed from NotI′ in reaction with **15** observed at 538.5 seconds; (G) Product formed from NotI′ in reaction with **15** observed at 526.0 seconds. Oxidized products have an expected $[M+H]^+$ of 452.2549. Data were measured on an Agilent Q-TOF LC-MS.

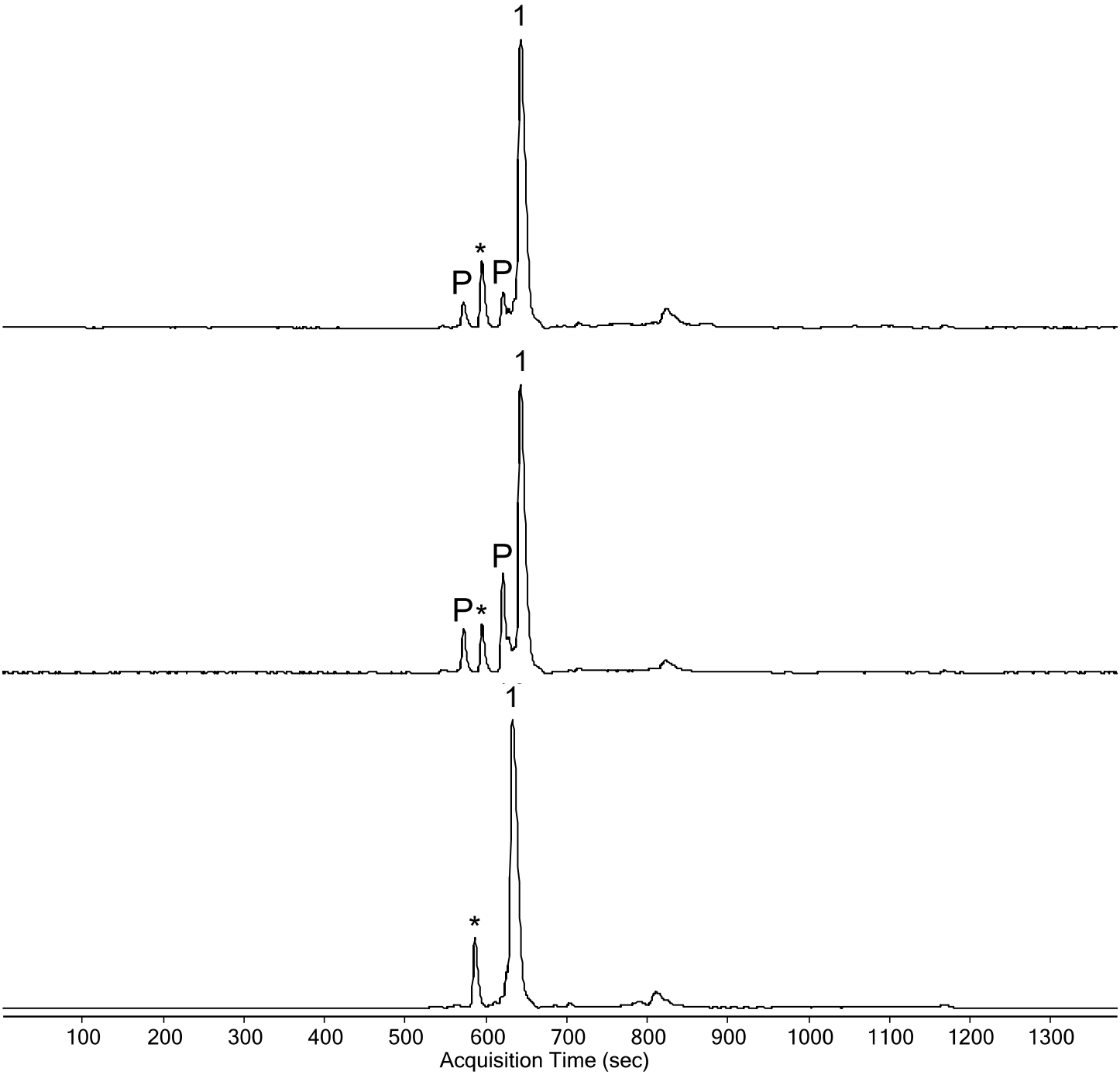

Figure S21. Q-TOF LC-MS analysis depicting EICs of (a) NotI′ reaction with notoamide E (**1**); (b) NotI reaction with **1**; (c) no enzyme control with **1**. Products formed are denoted with **P**. Asterisk denotes possible diastereomer of **1**. Data were measured on an Agilent Q-TOF LC-MS.

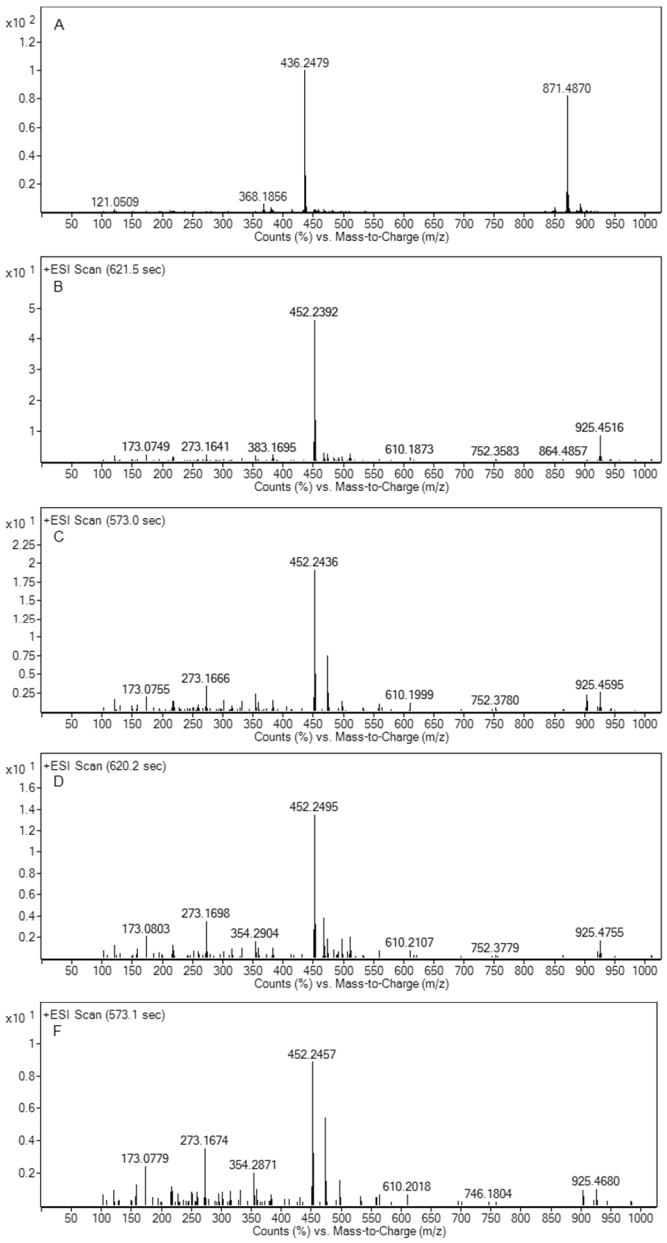

Figure S22. Mass spectra of (A) notoamide E (**1**) standard labelled with two ^{13}C atoms, expected $[M+H]^+$ = 436.2444; (B) Product formed from reaction of NotI with **1** observed at 621.5 seconds; (C) Product formed from reaction of NotI with **1** observed at 573.0 seconds; (D) Product formed from reaction of NotI′ with **1** observed at 620.2 seconds; (E) Product formed from reaction of NotI′ with **1** observed at 573.1 seconds. Oxidized products have an expected $[M+H]^+$ of 452.2393. Data were measured on an Agilent Q-TOF LC-MS.

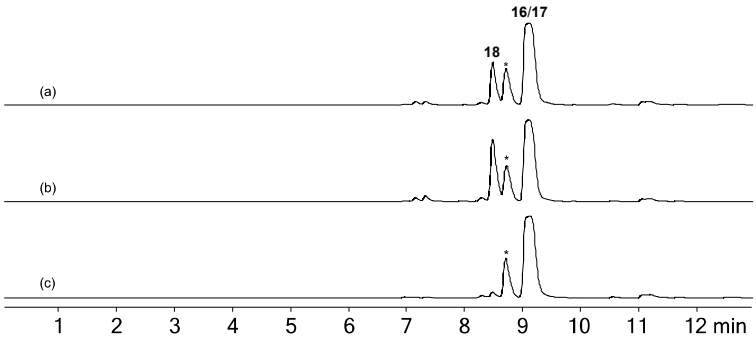

Figure S23. Q-TOF LC-MS analysis depicting EICs of (a) NotI reaction with notoamide T (**16/17**); (b) NotI′ reaction with **16/17**; (c) No enzyme control with **16/17**. Products formed are denoted with **18** (notoamide TI). Asterisk denotes possible diastereomers of **16**/**17**. Data were measured on an Agilent Q-TOF LC-MS.

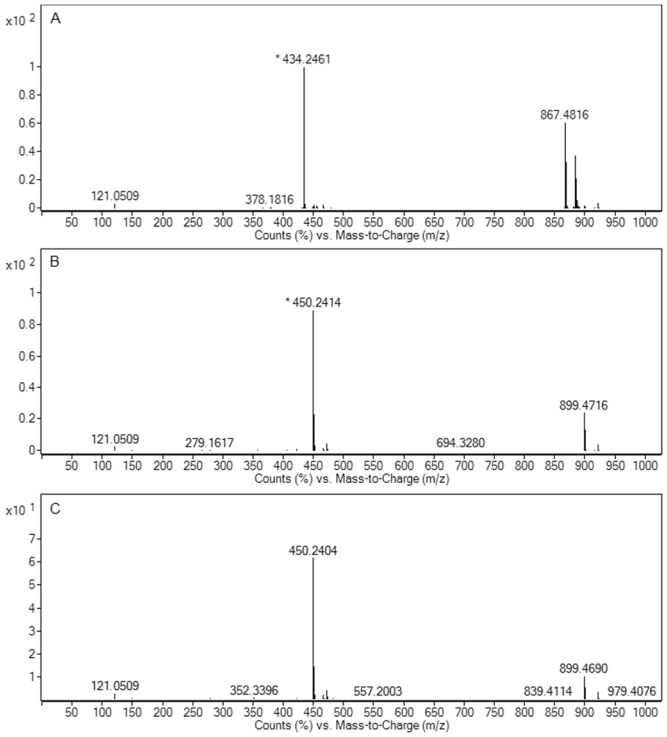

Figure S24. Mass spectra of (A) (+)- and (-)-notoamide T (**16** and **17**) standards in racemic mixture, expected $[M+H]^+$ = 434.2444; (B) Product formed from reaction of NotI with the racemic **16**/**17**, expected $[M+H]^+$ = 450.2392; (C) Product formed from reaction of NotI′ with the racemic **16**/**17**, expected $[M+H]^+$ = 450.2392. Data were measured on an Agilent Q-TOF LC-MS.

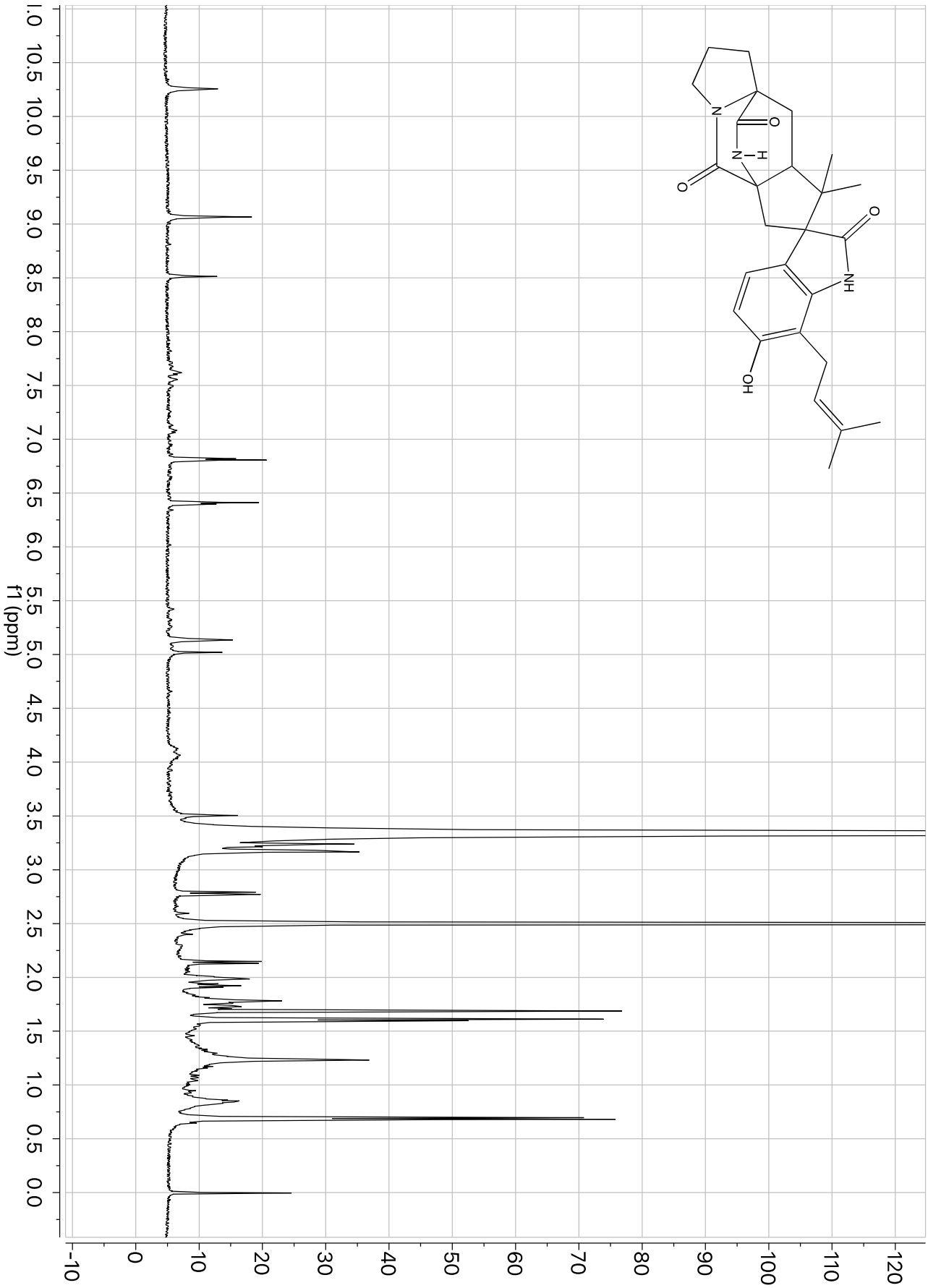

Figure S25. ^{1}H-NMR spectrum of Notoamide TI (**18**) recorded at 700 MHz in $(CD_3)_2SO$-d_6.

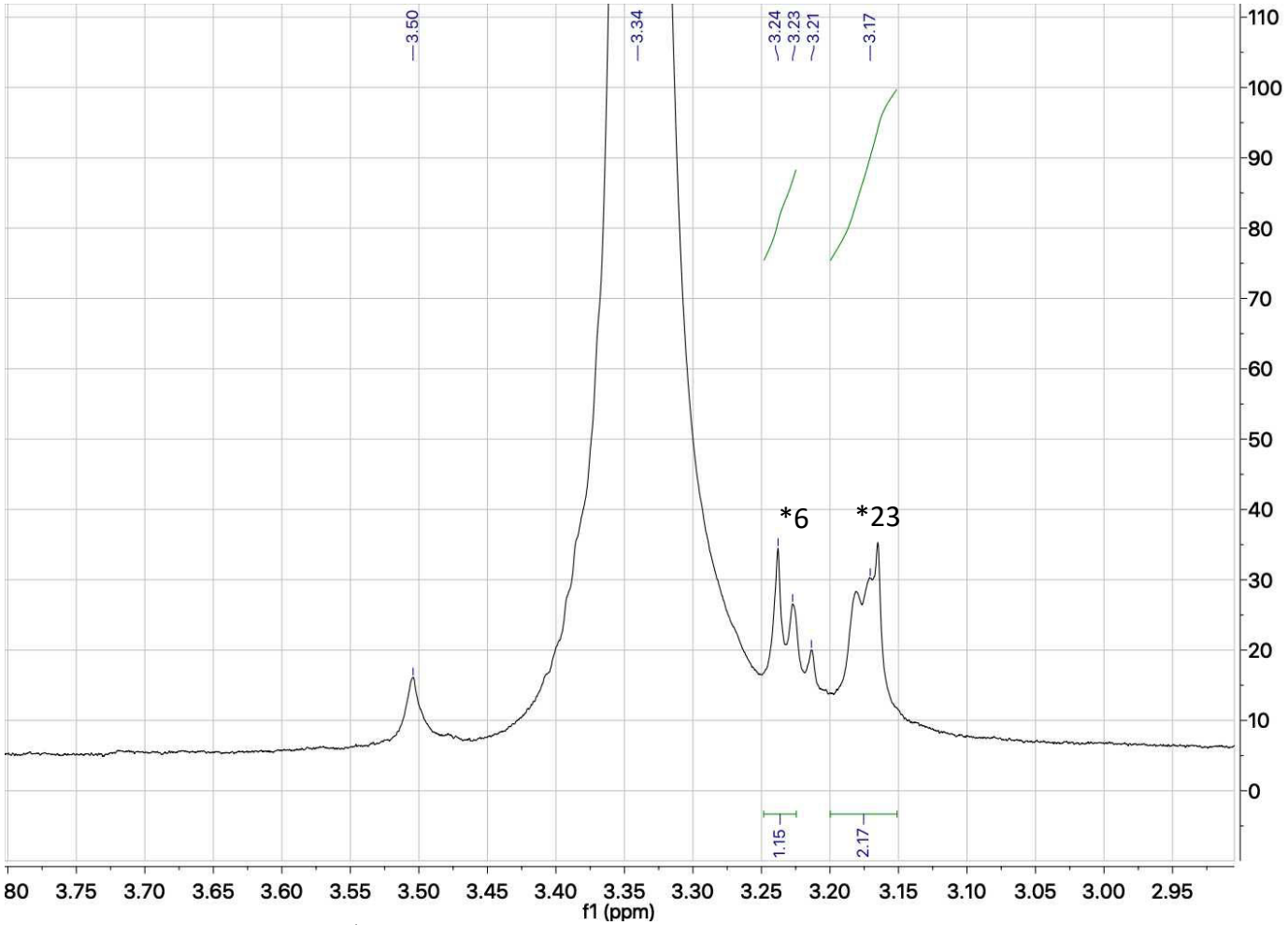

Figure S26. Zoomed view of ^{1}H-NMR spectrum of Notoamide TI (**18**) recorded at 700 MHz in $(CD_3)_2SO$-d_6 to show multiplets at 3.17ppm (CH_2, position 23) and 3.24ppm (CH, position 6).

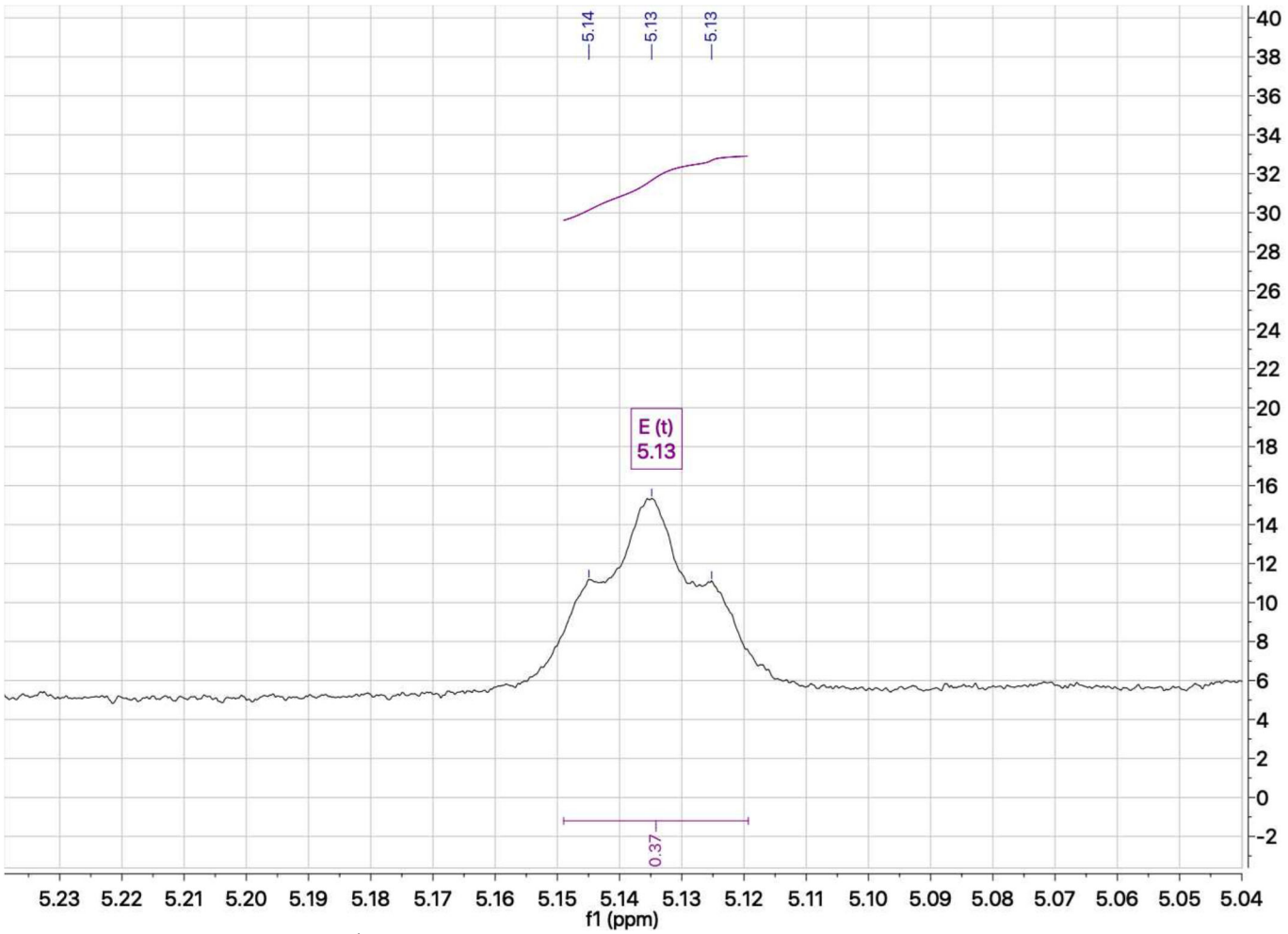

Figure S27. Zoomed view of ^{1}H-NMR spectrum of Notoamide TI (**18**) recorded at 700 MHz in $(CD_3)_2SO$-d_6 to show a triplet at 5.13 ppm (CH, position 24).

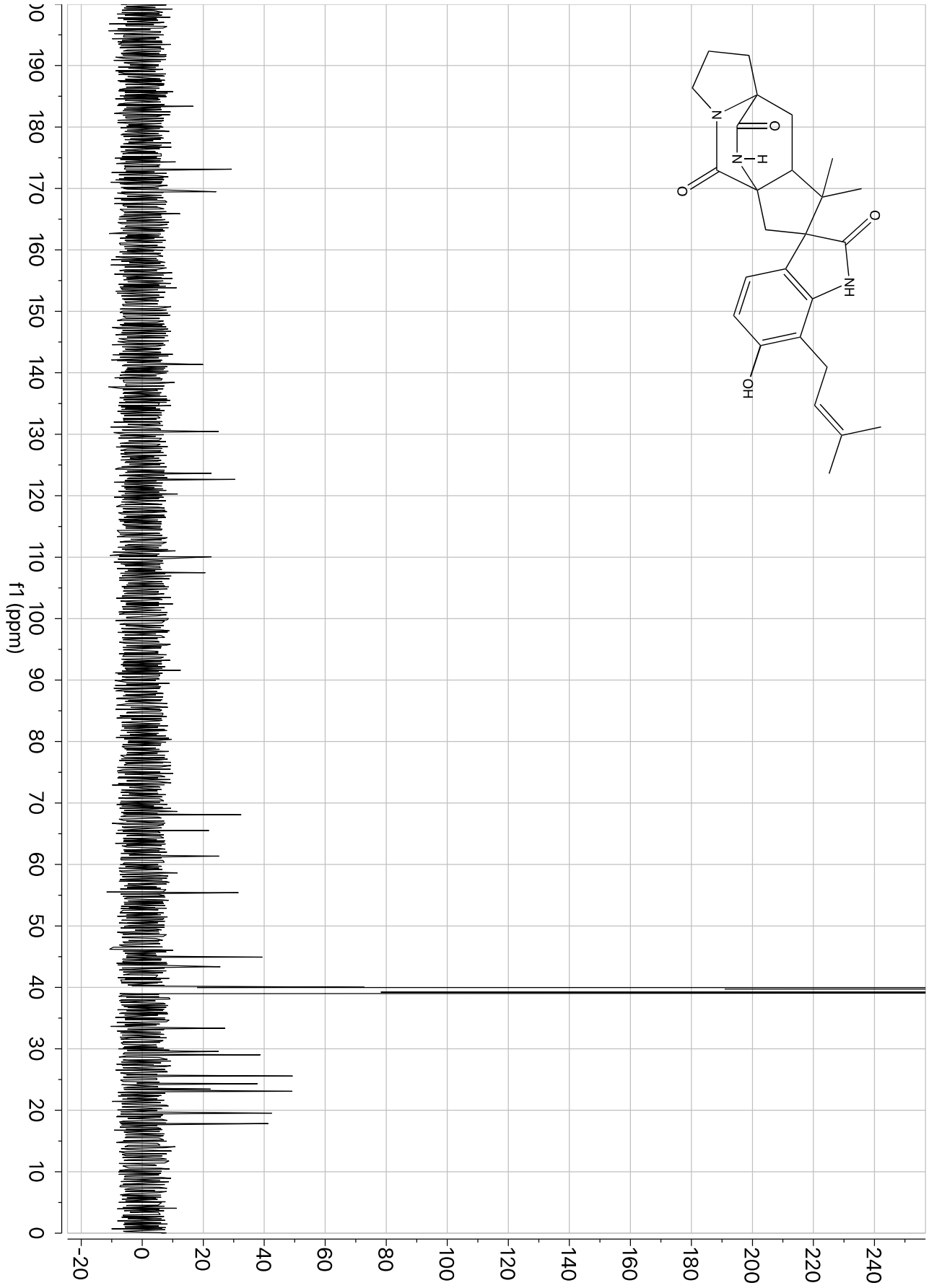

Figure S28. ^{13}C-NMR spectrum of Notoamide TI (**18**) recorded at 176 MHz in $(CD_3)_2SO$-d_6.

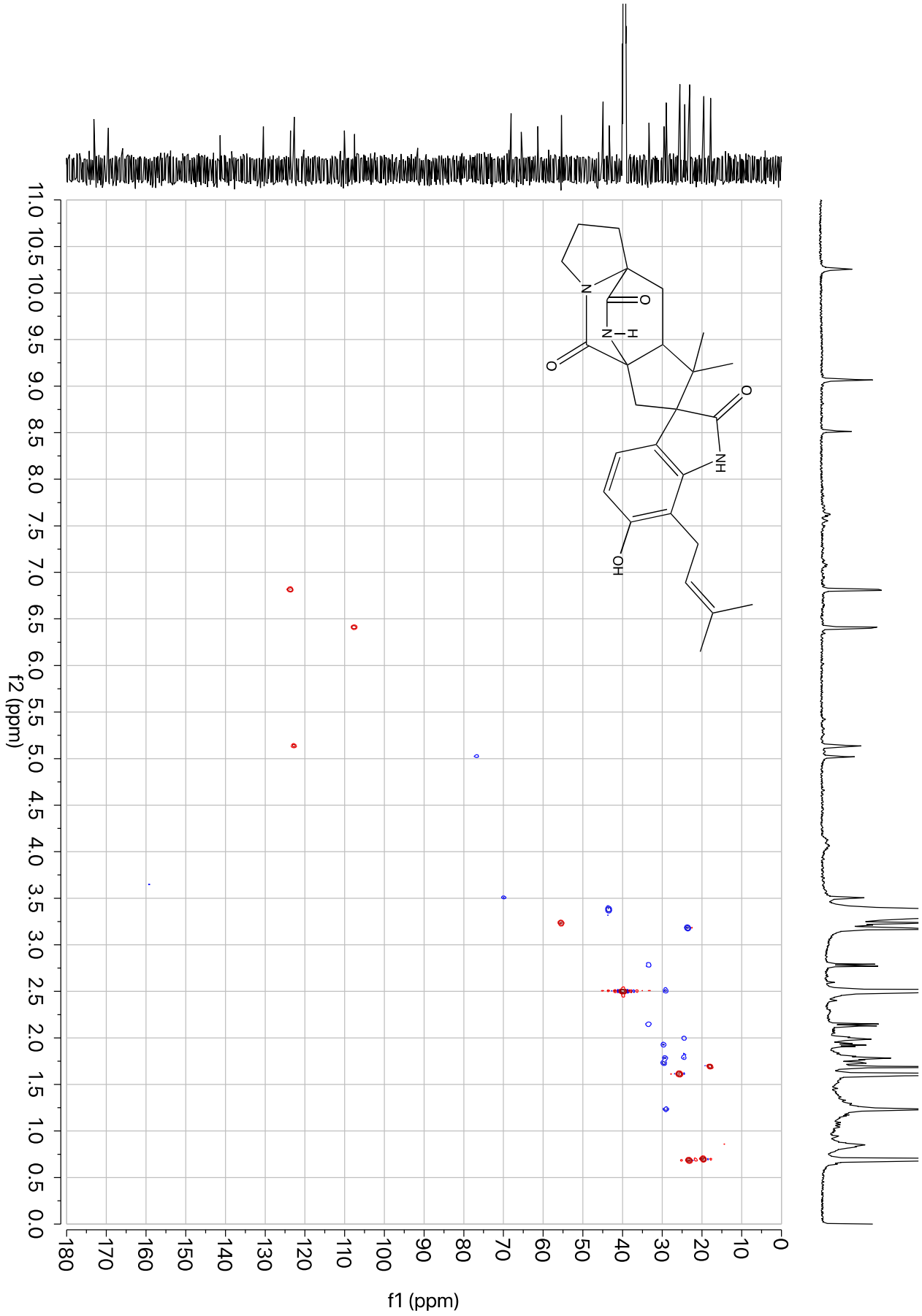

Figure S29. gHSQCAD spectrum of Notoamide TI (**18**) recorded at 700 MHz in $(CD_3)_2SO$-d_6.

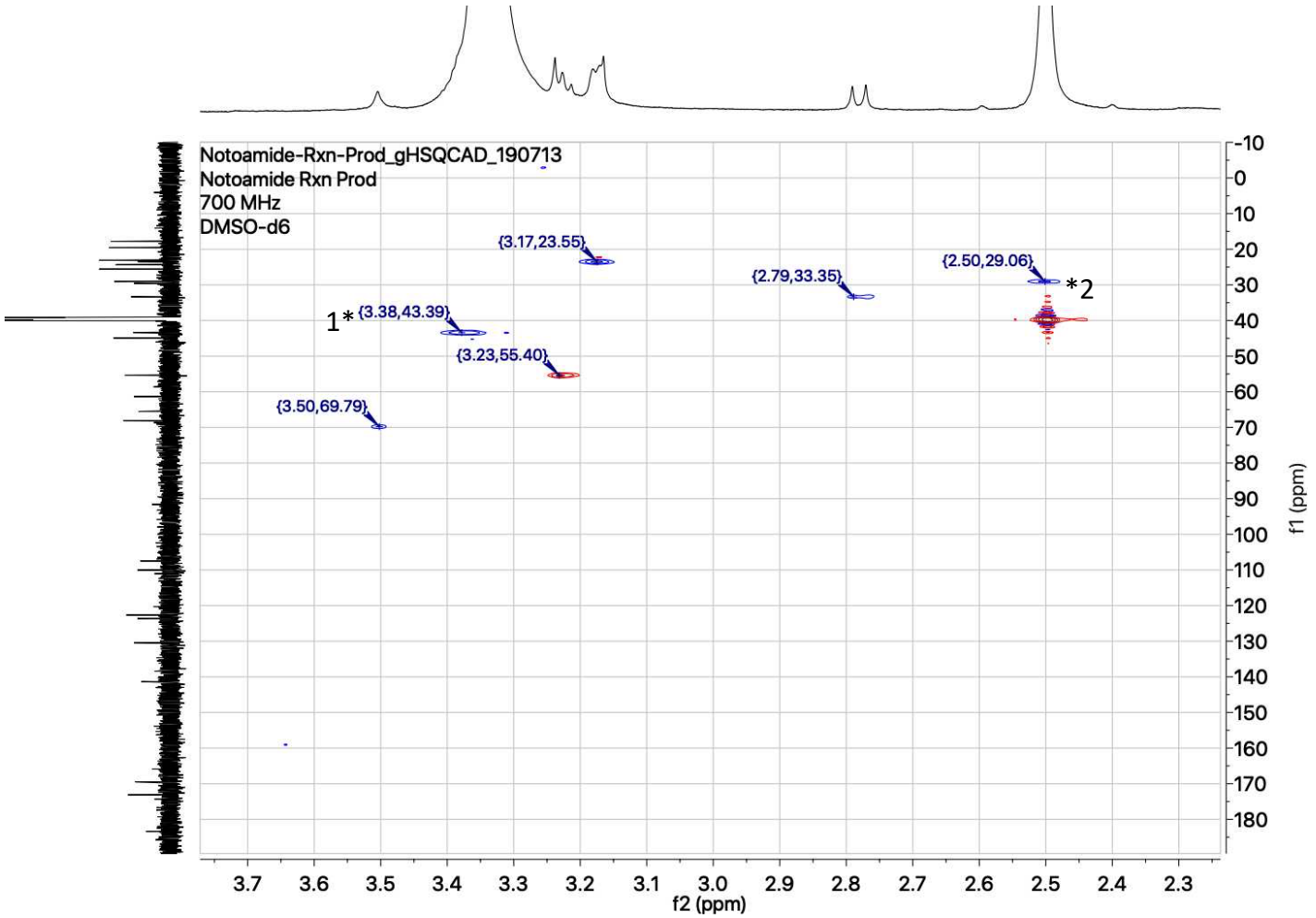

Figure S30. Zoomed view of the gHSQCAD spectrum of Notoamide TI (**18**) recorded at 700 MHz in $(CD_3)_2SO$-d_6 to display the solvent-obscured peaks at (C2, 2.50/29.06 ppm) and (C1, 3.38/43.39 ppm). The peaks for positions 2 and 1 are indicated with asterisks.

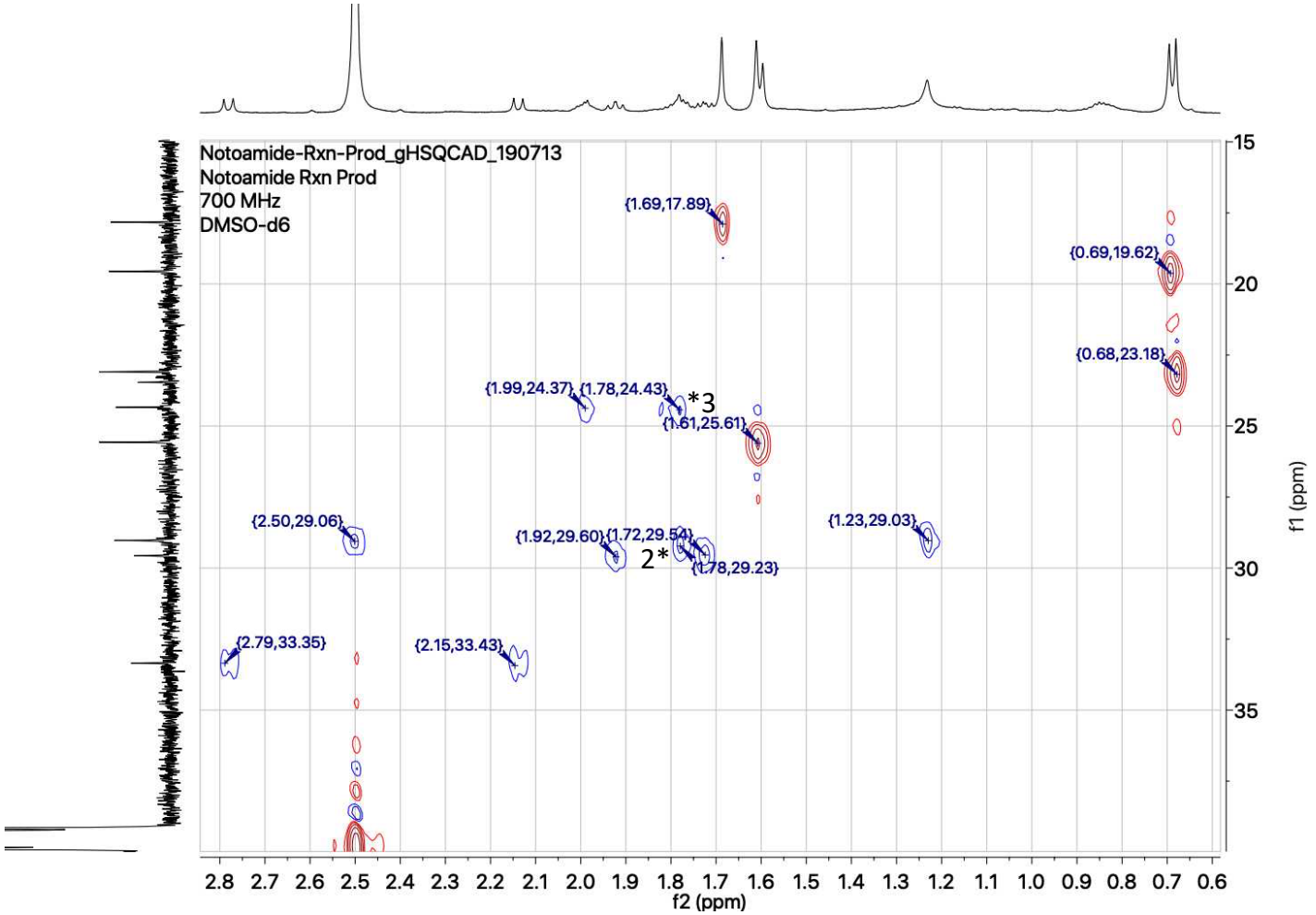

Figure S31. Zoomed view of the gHSQCAD spectrum of Notoamide TI (**18**) recorded at 700 MHz in $(CD_3)_2SO$-d_6 to display the peaks for C2 and C3, for which the proton signals overlap at 1.78. The peaks for positions 2 and 3 are indicated with asterisks.

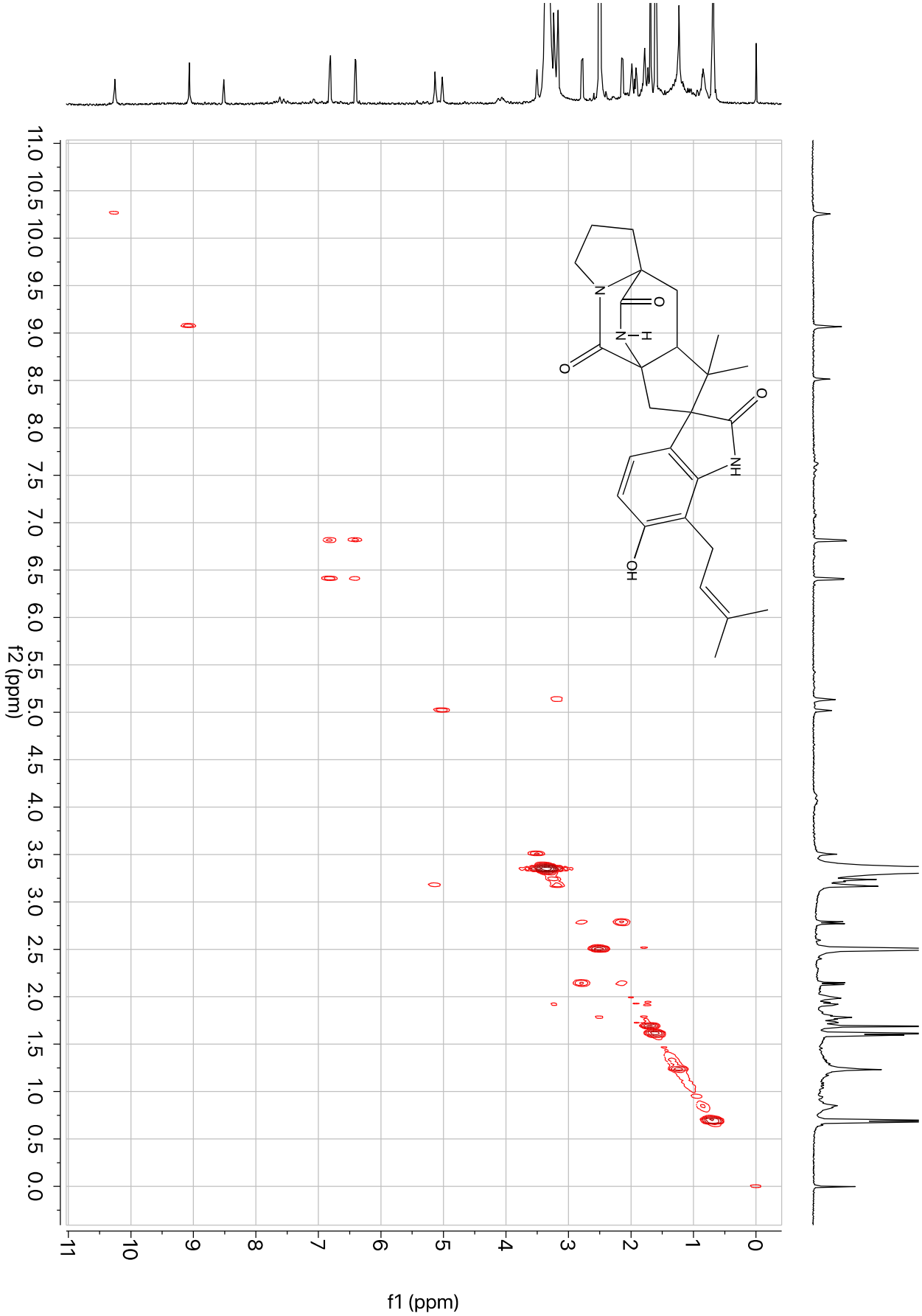

Figure S32. gCOSY spectrum of Notoamide TI (**18**) recorded at 700 MHz in $(CD_3)_2SO$-d_6.

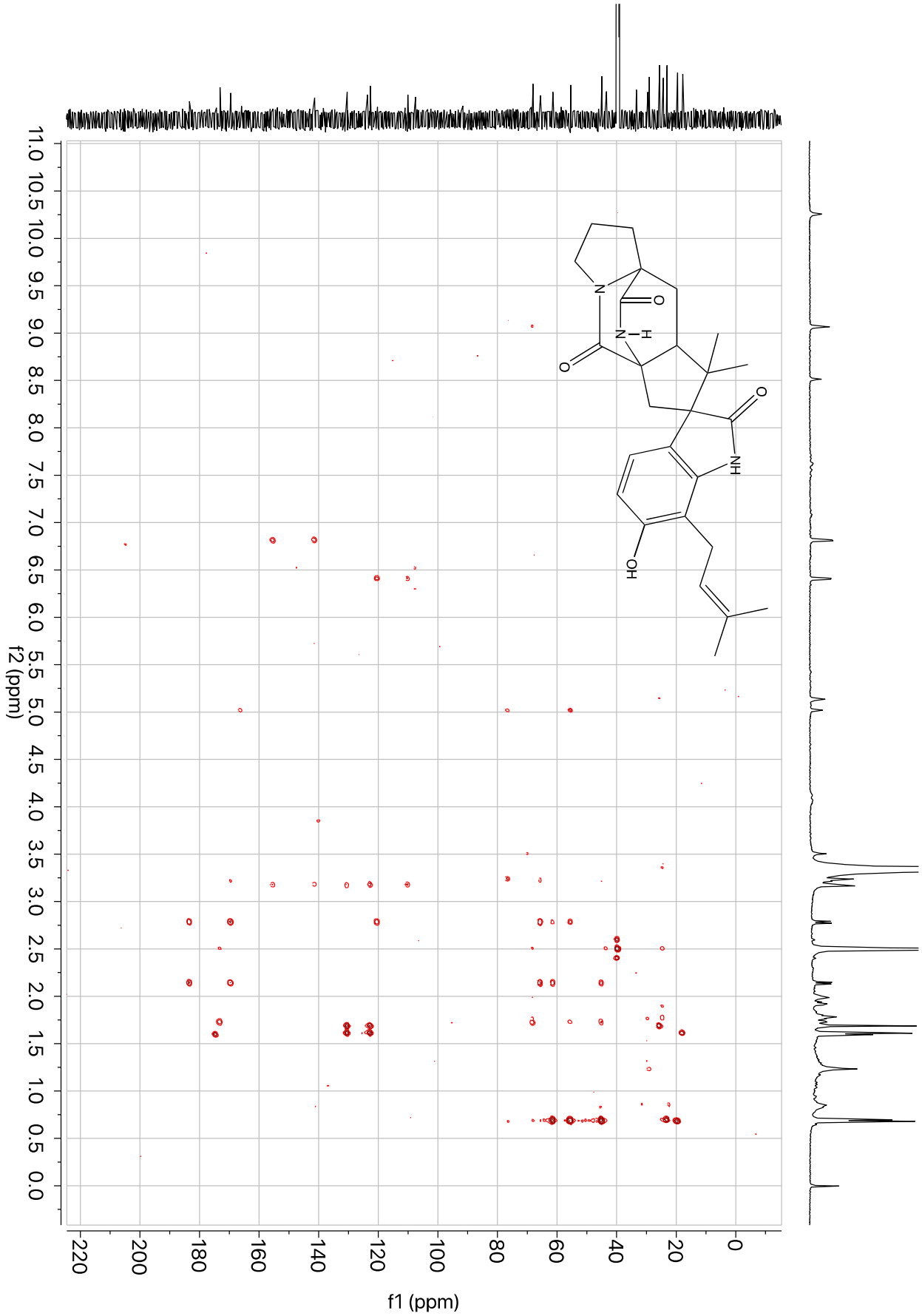

Figure S33. gHMBCAD spectrum of Notoamide TI (**18**) recorded at 700 MHz in $(CD_3)_2SO$-d_6.

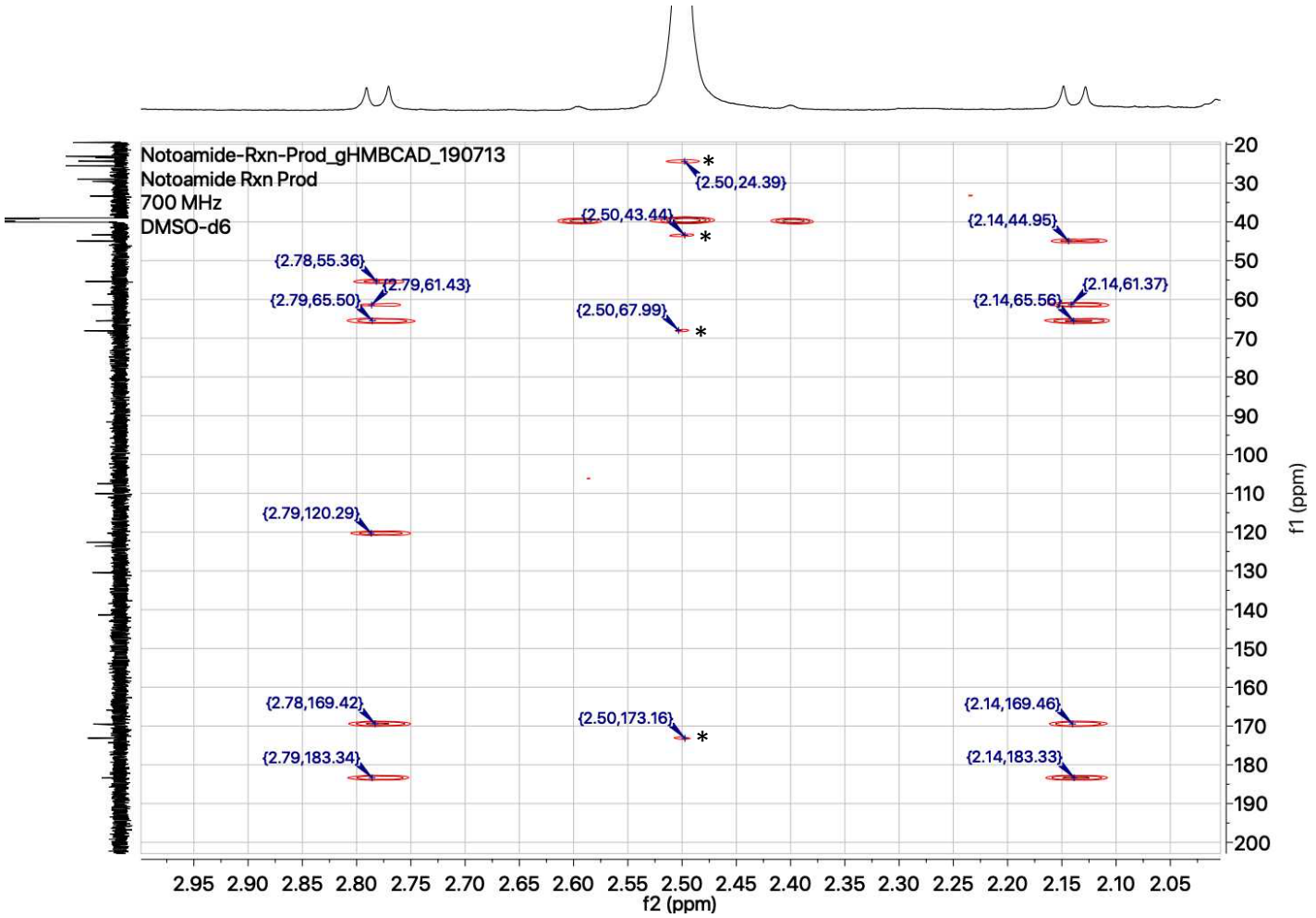

Figure S34. Zoomed view of the gHMBCAD spectrum of Notoamide TI (**18**) recorded at 700 MHz in $(CD_3)_2SO$-d_6 to display the correlations from the solvent-obscured peak at 2.50 ppm (indicated by asterisks).

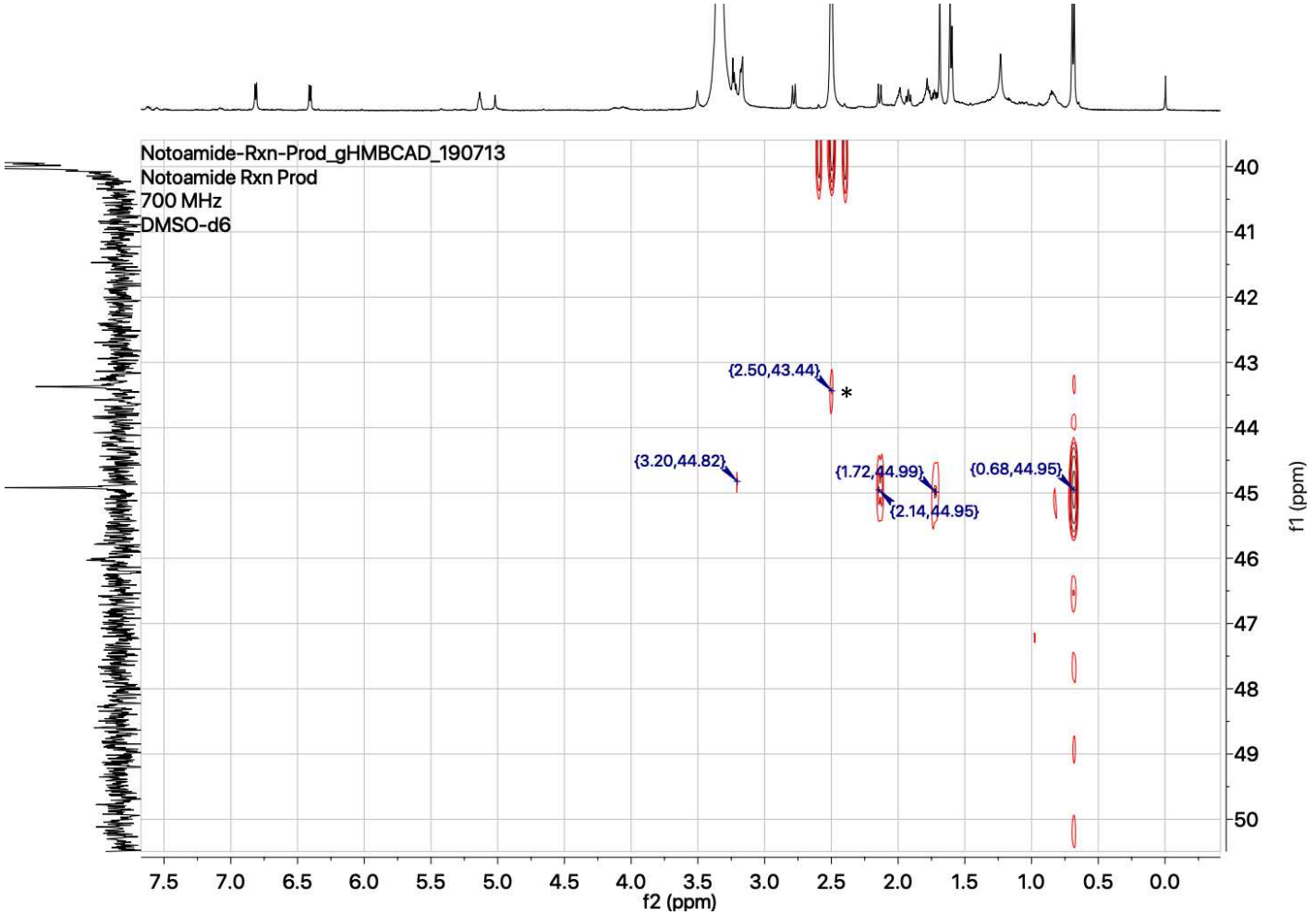

Figure S35. Zoomed view of the gHMBCAD spectrum of Notoamide TI (**18**) recorded at 700 MHz in $(CD_3)_2SO$-d_6 to display the correlations from the solvent-obscured peak at 2.50 ppm to C2, indicated by an asterisk.

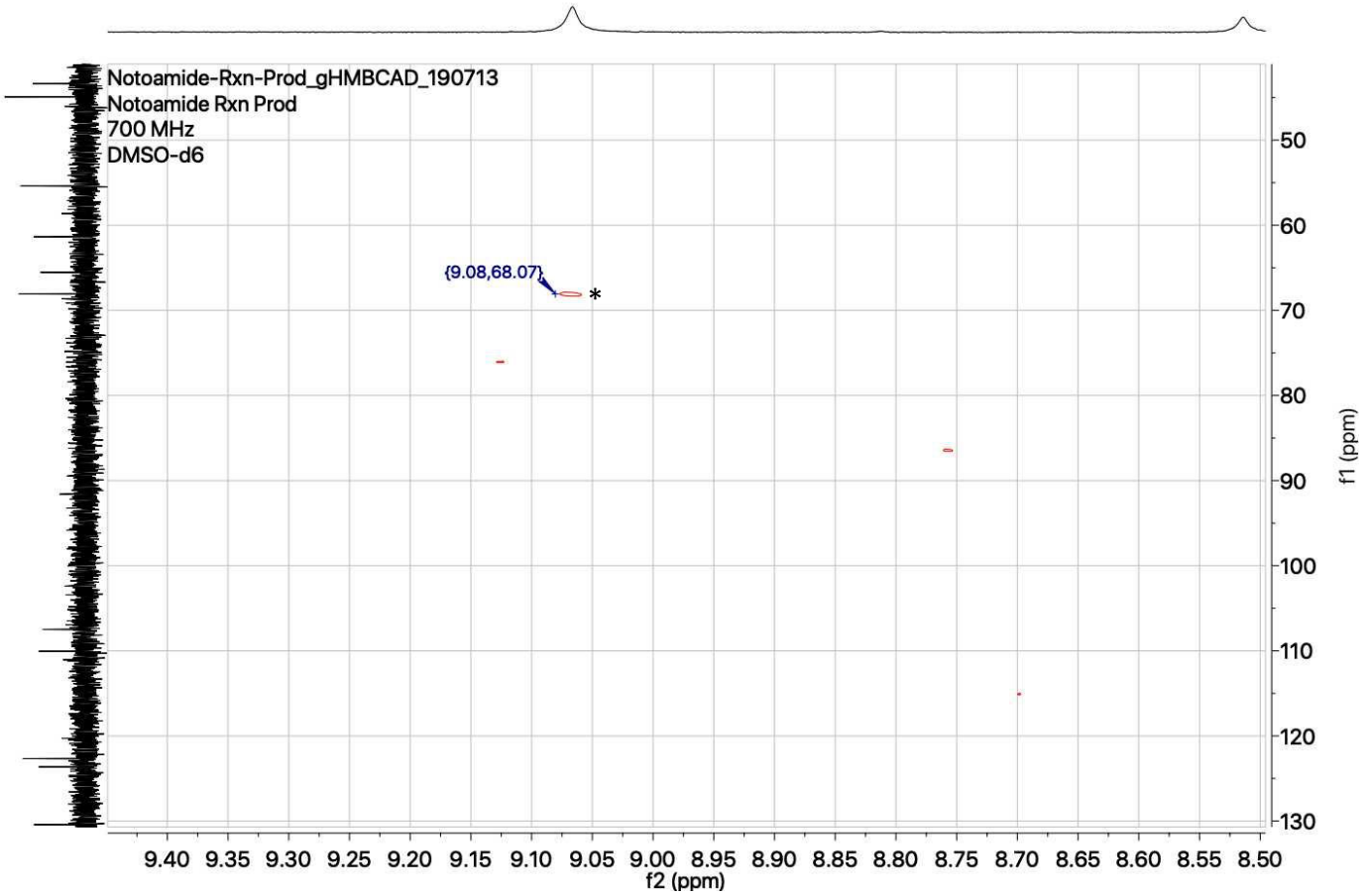

Figure S36. Zoomed view of the gHMBCAD spectrum of Notoamide TI (**18**) recorded at 700 MHz in $(CD_3)_2SO$-d_6 to display the correlations from NH(22) at 9.07ppm to C4 at 68.07ppm, indicated by an asterisk.